

Optical studies in distributed Bragg reflectors built from ZnO/MgO multilayer films

This content has been downloaded from IOPscience. Please scroll down to see the full text.

2013 Phys. Scr. 2013 014034

(<http://iopscience.iop.org/1402-4896/2013/T157/014034>)

View [the table of contents for this issue](#), or go to the [journal homepage](#) for more

Download details:

IP Address: 140.135.41.1

This content was downloaded on 03/12/2013 at 08:39

Please note that [terms and conditions apply](#).

Optical studies in distributed Bragg reflectors built from ZnO/MgO multilayer films

Y S Huang¹, C C Chang¹, J W Lee², Y C Lee³, C C Huang³, Z K Wun¹
and K K Tiong¹

¹ Department of Electronic Engineering, National Taiwan Ocean University, Keelung, Taiwan

² Department of Materials Engineering, Ming Chi University of Technology, Taishan, New Taipei City, Taiwan

³ Department of Electronic Engineering, Tunghan University, Shenkeng, New Taipei City, Taiwan

E-mail: jacklee@mail.tnu.edu.tw

Received 25 August 2012

Accepted for publication 18 December 2012

Published 15 November 2013

Online at stacks.iop.org/PhysScr/T157/014034

Abstract

We present the distributed Bragg reflectors (DBRs) with 10- and 15-period zinc oxide (ZnO)/MgO multilayer films deposited on silicon by sputtering technology. The reflectivity for the 10-period ZnO/MgO stacks can reach to 91.4% and for the 15-period ZnO/MgO stacks can be increased to 98.7%. Furthermore, the transfer matrix method takes account of the Sellmeier equation and the random thickness model, plus it can well describe the measured reflectivity spectra. The investigation indicates that a refined control of the individual layer thickness and the number of layer periods are significant subjects to improve the DBRs performance.

PACS numbers: 73.61.Ga, 78.67.Pt, 68.65.Ac

(Some figures may appear in color only in the online journal)

1. Introduction

Zinc oxide (ZnO) is a favorable II–VI semiconductor with a wide band gap of 3.37 eV and an exciton binding energy of 60 meV at room temperature. Up to now, ZnO and its ternary alloys have been of substantial interest due to their potential for optical and electronic device applications, such as solar cells, light emitters, sensors, modulators and UV detectors [1, 2]. So far, an interesting application for ZnO-based materials is in the distributed Bragg reflectors (DBRs), which can be incorporated into a vertical cavity surface emitting laser (VCSEL) [3].

The structure of DBRs consists of a sequence of alternating layers of two different materials, each of which has a thickness of $\lambda/4n$ (where λ is the designed resonant wavelength of the stop band and n is the refractive index of the material). For designing the DBRs structure, the value of the reflectivity and the width of the stop-band have to be considered. The reflectivity of DBRs would be influenced by the difference between the refractive indices (Δn) of the two layer materials and the numbers of periods (N) in the DBRs

stack. Additionally, the performance of the stop-band is the important characteristic of DBRs and it depends strongly on the value of Δn and the thicknesses of the two alternating layers [4].

In this work, the ZnO and MgO materials that have a wide-band-gap are selected for constructing DBRs structure, which can be incorporated into the short wavelength VCSEL. Moreover, the difference between the maximum refractive indices of ZnO and MgO material can be about 0.4, which is suitable for the DBRs structure. We have successfully deposited 10- and 15- period ZnO/MgO multilayer films on Si substrate by sputtering technology and measured the reflectivity spectra of the prepared samples. The measured reflectivity spectra are discussed by comparing with the simulation curves calculated using the transfer matrix method.

2. Experimental

Figure 1 shows the schematic diagram of ZnO/MgO multilayer films. To avoid complications in the

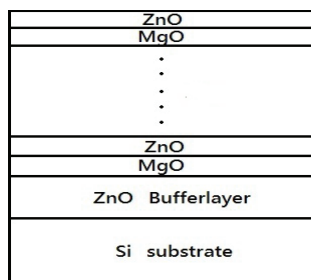


Figure 1. Schematic diagram of ZnO/MgO multilayer films.

Table 1. Detailed deposition parameters for MgO/ZnO multilayer thin films.

| | ZnO | MgO |
|----------------------------|-----------------------------|-----|
| Substrate | Si | |
| Target | ZnO | Mg |
| Gas flow (sccm) | Ar: 25, O ₂ : 25 | |
| Working pressure (Torr) | 10 ⁻³ | |
| Sputtering method | dc | RF |
| Sputtering power (W) | 50 | 150 |
| Substrate temperature (°C) | 300 | |

DBRs performance due to absorption, the resonant wavelength of the ZnO/MgO multilayer films was designed to be at 550 nm. The refractive indices of ZnO and MgO was derived from the Sellmeier equation ($n_{\text{ZnO}} = \sqrt{1 + \frac{2.60 \times \lambda^2}{\lambda^2 - 211.4^2}}$ and $n_{\text{MgO}} = \sqrt{1 + \frac{1.86 \times \lambda^2}{\lambda^2 - 100.4^2}}$) [5, 6], thus the $n_{\text{ZnO}} = 2.013$ and $n_{\text{MgO}} = 1.710$ were used. The desired thickness of an individual layer of ZnO and MgO was calculated to be 68.3 and 80.5 nm, respectively.

The ZnO/MgO multilayer films were deposited on p-type (100) silicon wafer substrates by a reactive magnetron sputtering system. The direct current (dc) and radio frequency (RF) power supplies were connected to a ZnO compound target and a pure Mg target, respectively. The diameter and thickness of each target were 76.2 and 6.0 mm, respectively. The substrate-to-target distance was kept at 85 mm. A base pressure of 6.65×10^{-4} Pa was achieved before sputtering and the working pressure during sputtering was 1.73×10^{-1} Pa. The flow rate of Ar : O₂ at a ratio of 1 : 1 was monitored by individual mass flow controllers.

All substrates were heated to 300 °C and rotated at a speed of 20 rpm during the sputtering process. The 300 nm thick ZnO buffer layer was deposited on the Si substrate first and then the desired thickness MgO layer and ZnO layer were sequentially deposited to fabricate the 10- and 15-period ZnO/MgO multilayer films. Detailed deposition parameters are listed in table 1.

The phases of thin films were explored by a glancing angle x-ray diffractometer (GA-XRD, PANalytical, X'pert, Holland) with an incidence angle of 1°. Cu K α radiation generated at 30 kV and 20 mA from a Cu target was used. The cross-section morphology was obtained by field emission scanning electron microscope (FE-SEM, JSM-6701F, JEOL, Japan). The reflectivity spectrum of the ZnO/MgO multilayer films was measured at normal incidence using a xenon lamp as the light source. The reflected beam was dispersed through a 0.5 m spectrometer (Zolix omni- λ 500) with a grating of

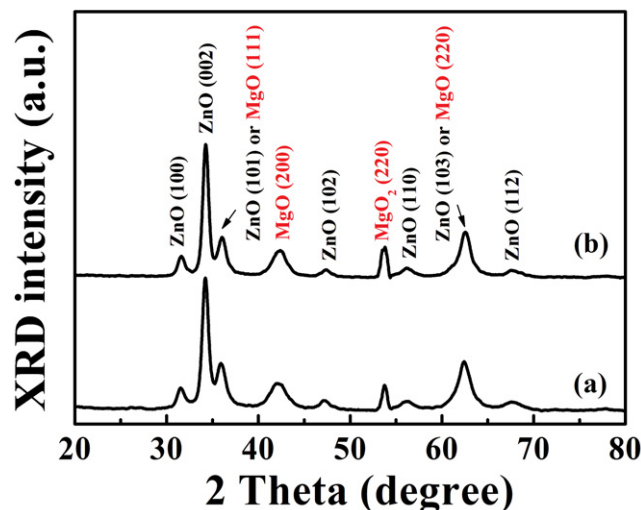


Figure 2. The XRD diffraction patterns of ZnO/MgO multilayer films with (a) 10- and (b) 15-period.

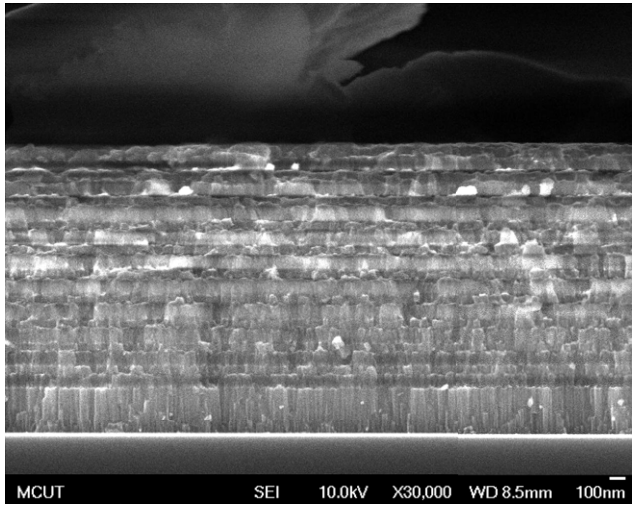
1200 grooves mm⁻¹ and detected using a photomultiplier tube.

3. Results and discussion

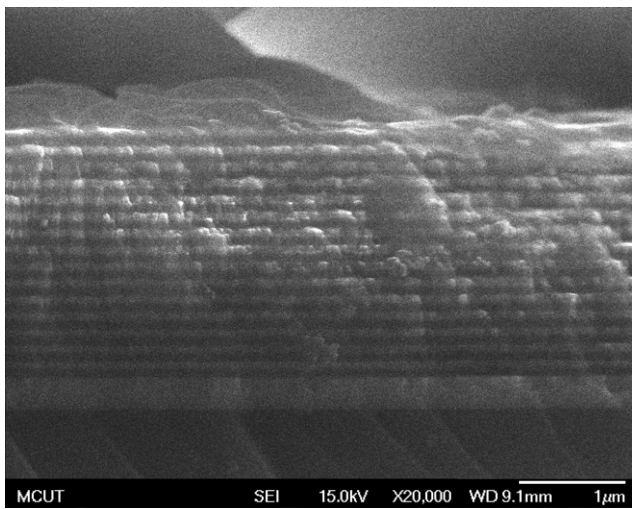
Figures 2(a) and (b) show the XRD diffraction patterns of the 10- and 15-period ZnO/MgO multilayer films, respectively. Referred to as JCPDS no. 89-7102 [7], the XRD signals at 31.7°, 34.4°, 36.2°, 47.5°, 56.6°, 62.8° and 67.9° are assigned to the (100), (002), (101), (102), (110), (103) and (112) of ZnO. According to JCPDS no. 89-7746 [8], the peaks at 36.8° and 62.1° can also be assigned to the (111) and (220) of the MgO material. The peaks at 42.8° and 53.5° are attributed to the typical signals for the MgO (200) and MgO₂ (220) [9], respectively. The XRD results show that the 10- and 15-period ZnO/MgO multilayer films have been fabricated successfully.

The cross-sectional SEM morphologies of the 10- and 15-period ZnO/MgO multilayer films are shown in figures 3(a) and (b), respectively. The images can exhibit the clear laminated structure and illustrate the multilayer microstructure consisting of bright ZnO and gray MgO layers. From the SEM images, the average thickness values of each of the ZnO and MgO layers are estimated to be about 69.6 and 72.3 nm for the 10-period ZnO/MgO stacks and about 75.9 and 73.5 nm for the 15-period ZnO/MgO stacks. It can be observed that the grown thickness of the ZnO and MgO layer is different from the designed thickness. The results can be explained by the fact that it is difficult to control the growth rate of a nanolayer during sputtering. In addition, the SEM images also show that the interface between the ZnO and MgO layer exhibits as a manifestation of waviness, which can be due to the large lattice mismatch between ZnO and MgO materials [4].

The reflectivity spectra of the 10- and 15-period ZnO/MgO multilayer films are measured and shown as opened dots in figures 4 and 5, respectively. The spectrum shows an asymmetric shape for the 10-period ZnO/MgO multilayer films, which tends to become symmetric for the 15-period ZnO/MgO multilayer films. In addition, the reflectivity is about 91.4% for the 10-period ZnO/MgO stacks



(a)



(b)

Figure 3. The cross-sectional SEM micrographs for the (a) 10- and (b) 15-period ZnO/MgO multilayer films.

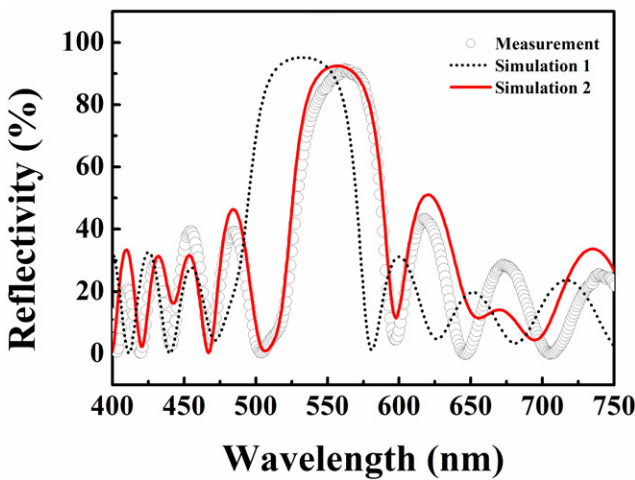


Figure 4. Measured and simulated reflectivity spectrum of the 10-period ZnO/MgO multilayer.

and can be increased effectively to 98.7% for the 15-period ZnO/MgO stacks; this evidences that the DBRs reflectivity is affected significantly by the number of periods. However,

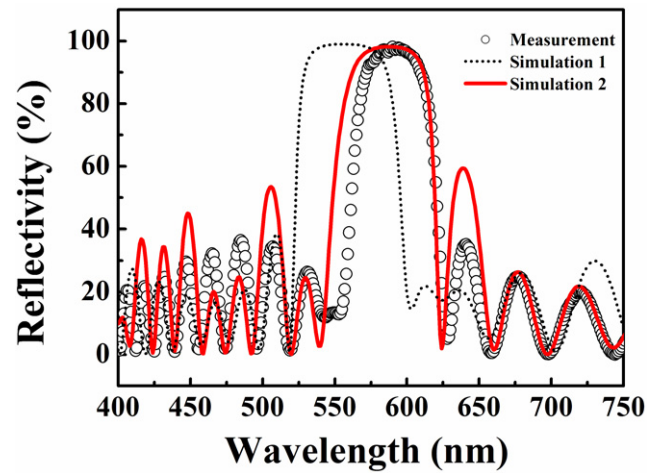


Figure 5. Measured and simulated reflectivity spectrum of the 15-period ZnO/MgO multilayer.

the stop-band center of the 10- and 15-period ZnO/MgO multilayer films is about at 561 and 597 nm, respectively, which deviates from the designed resonant wavelength. To clarify the discrepancy between the theoretical design and measured spectra, the simulated curves for multi-layer structures are investigated by the transfer matrix method [10]

$$\begin{pmatrix} M_{11} & M_{12} \\ M_{21} & M_{22} \end{pmatrix} = D_0^{-1} [D_H \cdot P_H \cdot D_H^{-1} \cdot D_L \cdot P_L \cdot D_L^{-1}]^N D_S, \quad (1)$$

where $D = \begin{bmatrix} 1 & 1 \\ n & -n \end{bmatrix}$ and $P = \begin{bmatrix} e^{i\varphi} & 0 \\ 0 & -e^{i\varphi} \end{bmatrix}$ ($\varphi = \frac{2\pi nd}{\lambda}$, d is thickness); thus D_0 , D_H , D_L and D_S are the dynamic matrices for free space, ZnO, MgO and Si substrate, respectively; P_H and P_L are the propagation matrices for ZnO and MgO, respectively; N is the number of periods.

The dotted lines shown in figures 4 and 5 are the simulation curves (simulation 1), which are calculated using the constant refractive index values of $n_{ZnO} = 2.013$ and $n_{MgO} = 1.710$ and the average layer thickness of the ZnO and MgO layers obtained from the SEM images. It is noted that the simulation 1 curves do not fit the experimental spectra. To understand the discrepancy between the simulated and experimental spectra, two important characteristic factors: the refractive index and layer thicknesses, have to be considered. It is known that the refractive index depends on the wavelength, hence the wavelength-dependent refractive index (as mentioned above) is used instead of the constant refractive index value ($n_{ZnO} = 2.013$ and $n_{MgO} = 1.710$). On the other hand, the SEM images show that the growth thicknesses of the individual ZnO or MgO layer are not uniform, implying that the average layer thicknesses are not suitable to be substituted into equation (1). Murtaza and Campbell [11] investigated the effects of changes in layer thicknesses during a growth run on reflectivity spectra and took account of the model of distributed random thickness in the transfer matrix method. According to the model of distributed random thickness, we use a random number generator to generate modified thicknesses, with a nominal thickness equal to the designed thickness and standard deviations 10% of the designed thicknesses, respectively.

The re-calculated curves (simulation 2) that take account of the wavelength-dependent refractive index and the distributed random thickness are displayed as the red solid lines in figures 4 and 5. It exhibits that the simulation 2 curves fit well to the measured data, which evidences that both the refractive index and layer thicknesses would significantly affect the performance of DBRs.

4. Conclusion

In summary, we have successfully fabricated 10- and 15-period ZnO/MgO multilayer films on Si by sputtering technology for a DBRs structure with a design resonant wavelength of 550 nm. The 10-period ZnO/MgO stacks have 91.4% reflectivity; the reflectivity can be increased to 98.7% by increasing the ZnO/MgO stacks to a 15-period. It is found that the growth thicknesses of the individual ZnO and MgO layers deviate from the designed thicknesses; the random variations in layer thicknesses can result from different sources of error in the growth and control apparatus. Both the wavelength-dependent refractive index and the distributed random thickness have to be taken into account in the transfer matrix method to describe the measured reflectivity spectra, which can interpret the deviations from an ideal structure resulting in the distortion and the shifting of the reflectivity spectrum. We present that a more refined control of the individual layer thickness and the number of layer periods can further improve the Bragg structures.

Acknowledgment

The author acknowledges the support of the National Science Council Project no. NSC 99-2112-M-236-001-MY3.

References

- [1] Lorenz M, Hochmuth H, Schmidt-Grund R, Kaidashev E M and Grundmann M 2004 *Ann. Phys., Lpz.* **13** 59
- [2] Wang Z Y, Hu L Z, Zhao J, Zhang H Q and Wang Z J 2006 *Vacuum* **80** 977
- [3] Roux C, Hadji E and Pautrat J L 1999 *Appl. Phys. Lett.* **75** 1661
- [4] Peiris F C, Lee S, Bindley U and Furdyna J K 1999 *Semicond. Sci. Technol.* **14** 878
- [5] Teng C W, Muth J F, Özgür Ü, Bergmann M J, Everitt H O, Sharma A K, Jin C and Narayan J 2000 *Appl. Phys. Lett.* **76** 979
- [6] Chen N B, Wu H Z and Xu T N 2005 *J. Appl. Phys.* **97** 023515
- [7] Barros T S, Barros B S, Alves S Jr, Kiminami R H A G, Lira H L and Costa A C F M 2008 *Mater. Sci. Forum* **591** 745
- [8] Sundraraja M, Suresh J and Rajiv Gandhi R 2012 *Dig. J. Nanomater. Biostruct.* **7** 983
- [9] Nakano S, Yamaura S I, Kitano A, Sato M, Uchinashi S, Hamada T, Umesaki N, Kimura H and Inoue A 2004 *Mater. Trans.* **45** 3232
- [10] Shen J L, Chang C Y, Chen P N, Chou W C, Chen Y F and Wu M C 2001 *Opt. Commun.* **199** 155
- [11] Murtaza S S and Campbell J C 1995 *J. Appl. Phys.* **77** 3641